Songklanakarin J. Sci. Technol.
43 (1), 229-236, Jan. - Feb. 2021

http://www.sjst.psu.ac.th

Original Article

Development of solid tire model for finite element analysis of compressive loading

Juthanee Phromjan[1, 2] and Chakrit Suvanjumrat[1, 2*]

[1] *Department of Mechanical Engineering, Faculty of Engineering, Mahidol University, Phutthamonthon, Nakhon Pathom, 73170 Thailand*

[2] *Laboratory of Computer Mechanics for Design (LCMD), Department of Mechanical Engineering, Faculty of Engineering, Mahidol University, Phutthamonthon, Nakhon Pathom, 73170 Thailand*

Received: 25 December 2019; Revised; 11 July 2019; Accepted: 13 January 2020

Abstract

A solid tire model for forklift trucks has been developed in order to investigate tire performance while supporting a compressive load. The rubber compounds used for solid tire layers were tested to obtain their stress-strain characteristics and to assess applicability of a constitutive model. The Ogden model was suitable for representing the stress-strain characteristics in all layers of a solid tire. The three-dimensional finite element model of a solid tire was developed by assembling the internal, middle, and tread layers. In order to validate this solid tire model, compression load tests were performed on simulated solid tires. The deflection and footprint results of the simulations were found to agree well with experimental data, with an average error less than 10.31%.

Keywords: compression load, finite element analysis, footprint, solid tire

1. Introduction

The solid tires that are used with forklift trucks are excellent for supporting heavy loads. The components of a solid tire are an internal layer, a middle layer, a tread layer, and steel wires for the three-rubber-layer tire. Nowadays, computer-aided design (CAD) and computer-aided engineering (CAE) are widely employed to develop and design tires. Finite elements have been widely used to simulate and determine the best characteristics of these. Using the finite element method (FEM) can reduce the cost and time consumption of trial and error design methods. Behroozi, Olatunbosun, and Ding, (2012) have developed a complex aircraft tire model using FEM. That model was used to predict the tire behavior. Guo, Bastien, Blundell, and Wood, (2014) also used FEM to develop an aircraft tire model. Their model has been effectively used during the tire design process. To obtain accurate results from FEM, the constitutive model chosen is an important factor in describing the deformation behavior of the rubber compounds. Constitutive models that are widely used to analyze the tire performance and to represent the deformation behavior include the Mooney-Rivlin, the Arruda-Boyce, the Yeoh, and the Ogden models. Baranowski, Mala chowski, Janiszewski, and Wwkwzer, (2016) and Baranowski, Malachowski, and Mazur kiewicz, (2016) performed multistage testing for validation of the finite element model of truck tire, comparing both deformation and failure. The Ogden model with small inaccuracy at a low strain rate was used in Quasi-static test, and it was indicated that the results were acceptable. Particularly, Baranowski, Janiszewsk, and Malachowski, (2017) found that the tested tire rubber is weakly sensitive to small differences in strain rate by Quasi-static test at low strain. Mohsenimanesh, Ward, & Gilchrist, (2009) used the Mooney-Rivlin model to describe the deformation behavior of rubber materials and to analyze the contact pressure distribution in the tread of a radial tractor tire. Namjoo and Golbakhshi, (2015) studied the tire/road contact effect using FEM. The material properties of radial tire tread have been analyzed using the Mooney-Rivlin model. Yang and

*Corresponding author
Email address: chakrit.suv@mahidol.ac.th

Olatunbosun, (2012) have analyzed racing tire characteristics using FEM and the Yeoh model. The vertical stiffness of racing tires has been analyzed and optimized for the model. Li, Wei, Feng, & Luo, (2017) applied a polynomial model using two invariants to describe the stress-strain characteristic of Nylon 66 tire cord. Wei and Olatunbosun, (2016) selected the Yeoh model to investigate the pneumatic tire. They studied the tire structure layup and the material properties using FEM. They analyzed the cornering performance and relaxation length for a constant slip angle of the rolling tire. These analyses incorporated the stress-strain characteristics of tire materials. Actually, the tensile tests were carried out on thin rubber strips of the material components of such tires.

A key property of solid tires is compression strength, because the tires support heavy loads and are driven at a low speed. The compression test yields the stress-strain characteristics of the solid tire materials. Zhang and Zhang, (2016) have analyzed D-ring rubber using FEM. The Mooney-Rivlin model was chosen. This finite element model was used to analyze also the sealing performance. Zhou *et al.* (2017) also created an O-ring model for analyzing the seal capacity using FEM. The Mooney-Rivlin model has also been used to explain the deformation behavior of nitrile-butadiene rubber in an O-ring. Hassan, Abouel-Kasim, El-Sharief, and Yusof, (2012) compared seven constitutive models based on hyper-elastic material. The stress-strain characteristics of the nitrile butadiene rubber obtained from compression tests were used for the data fitting. Although such rubber materials have been described by the strain energy function, they differed from the constitutive model of a solid rubber tire. Consequently, simulation of the solid tire has not been widely used in the relevant industries to develop the current products.

This research has developed an approach for determining a constitutive model of those rubber compounds that are used to produce three-layer solid tires. The finite element analysis (FEA) of solid tires was developed for simulation of the compression test. Therefore, this model will be an advantage in developing good quality solid tires.

2. Finite Element Method

The solid tire deformation caused by an external load is governed by the following equations.

$$\frac{\partial \sigma_{ij}}{\partial x_j} + \gamma_i = 0 \tag{1}$$

And

$$\tau_i = \sigma_{ij} n_j \tag{2}$$

where σ_{ij} is Cauchy stress, x_j is Cartesian coordinate, γ_i is body force, and τ_i is the boundary traction component.

Equation (1) can be transformed using FEM (Bathe, 2014) and written as follows:

$$(\boldsymbol{K_E} + \boldsymbol{K_G})\Delta v = f_l + f_{int} \tag{3}$$

$$\boldsymbol{K_E} = \int \boldsymbol{B}^T C \boldsymbol{B} d\forall \tag{4}$$

$$\boldsymbol{K_G} = \int \left(L_{jpk} \cdot \sigma^0_{ki} \cdot L_{jqi} - 2B_{jpk} \cdot \sigma^0_{ki} \cdot B_{iqj}\right) d\forall \tag{5}$$

$$\boldsymbol{f}_l = \boldsymbol{f}_b + \boldsymbol{f}_{tract} = \int \boldsymbol{N}^T \gamma d\forall + \int \boldsymbol{N}^T \tau dS \tag{6}$$

$$\boldsymbol{f}_{int} = \int \boldsymbol{B}^T \sigma d\forall \tag{7}$$

where $\boldsymbol{K_E}$ is the elastic stiffness matrix, $\boldsymbol{K_G}$ is the geometry stiffness matrix, v is the nodal displacement, $\boldsymbol{f}_l$ is the external load vector, $\boldsymbol{f}_{int}$ is the internal load vector, C is a constant over the element, $\boldsymbol{B}$ is the strain interpolation matrix, V is the element volume, S is the element surface, L_{jpk} is the Cartesian different operator, and $\boldsymbol{N}$ is the shape function matrix.

The constitutive model in the FEA is contained within the elastic stiffness matrix function. The constitutive models of the hyper-elastic materials are explained using the strain energy function related to the stress-strain characteristics. The Ogden model proposes a strain energy function based on the principal stretches for incompressible materials (Ogden, 1972; 1997). The strain energy potential of the Ogden model is:

$$U = \sum_{i=1}^{n} \frac{\mu_i}{\alpha_i}\left(\bar{\lambda}_1^{\alpha_i} + \bar{\lambda}_2^{\alpha_i} + \bar{\lambda}_3^{\alpha_i} - 3\right) + 4.5K\left(J^{1/3} - 1\right)^2 \tag{8}$$

and

$$\bar{\lambda}_i = J^{1/3}\lambda_i, \qquad J = \lambda_1\lambda_2\lambda_3 \tag{9}$$

where λ_i is the deviatoric principal stretch, J is the Jacobian determinant, K is the initial bulk modulus, and μ_i, α_i are constants

3. Experimental

The compression test was set up for both rubber specimens and solid tires. The testing of specimens was performed in order to determine the stress-strain characteristics of the rubber compounds used. The compression tests of solid tires were performed to investigate the vertical deformation and footprint of actual solid tires.

3.1 Rubber compounds

The three-layer solid tires were produced by V.S. Industry Tyres Co., Ltd in Thailand. Figure 1 shows the assembly of a solid tire. It was assembled with three rubber layers and steel wires. Each layer of the solid tire involved different rubber compounds. The manufacturing codes of these compound were M058, M047, and M067 for the internal, middle and tread layers, respectively. The layers of a solid tire are difficult to cut for the preparation of specimen because they are very hard. Therefore, sample rubber compounds accorded to the tire layers were specially prepared for the compression test. This was done according to ASTM D575-91. They had diameter and thickness of 28.6 and 12.5 mm, respectively. Figure 2 shows a rubber compound specimen. Such specimens are smaller than the solid tires and consequently their curing time is less. In order to characterize the rubber compound curing, a moving die rheometer was used following ASTM D5289. The compression

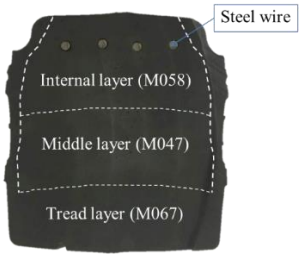

Figure 1. The cross-section of solid tire

Figure 2. The rubber compound specimen

testing of the specimens was done according to ASTM D575-91. There were six test pieces for each rubber compound. Each compression test was performed three times in order to reduce the Mullins effect. The vertical deformation of specimens was to -50% of the initial thickness. The final results of each test were used to characterize the stress-strain characteristics of the rubber compounds.

3.2 Solid tires

Solid tires, all branded KOMACHI, were studied in the compression test. The characteristic geometry of the KOMACHI solid tire is described in Table 1. The width and wheel size were 6 and 9 inches (6.00-9), respectively. A steel wheel with a diameter and E collar profile width of 9 and 4 inches (4.00E-9) was fitted to the solid tires. This was then mounted on the axle of the stiffness tester as shown in Figure 3(a). In order to measure the vertical deformation it was then loaded onto a measurement table, which had a displacement error of less than ±0.1 mm. The compression load was assigned at 4.0, 5.0, 6.0, 8.0, 10.0 and 12.0 kN. Because of the Mullins effect, each compression measuring the vertical displacement of the solid tire was gradually increased to the loading target three times. The final results of these compression load tests were used to evaluate the solid tire stiffness.

The footprint of KOMACHI solid tires was observed using a pressure measurement film. This was scanned and digitized by image processing software to calculate the footprint length, width, and area, for the contact pressure. Figure 3(b) presents the footprint characteristics of solid tire on pressure measurement film. The footprint area (FA) was calculated by w×l while the contact area (CA) was presented in red color. The footprint of the solid tire was observed under compression loads at 4.0, 5.0, 6.0, 8.0, 10.0 and 12.0 kN.

Table 1. The KOMACHI solid tire specifications

Size (inch)	Rim size (inch)	Tire dimension (mm)		Weight (kg)
		Section width	O.D.	
6.00-9	4.00E-9	145	523	27

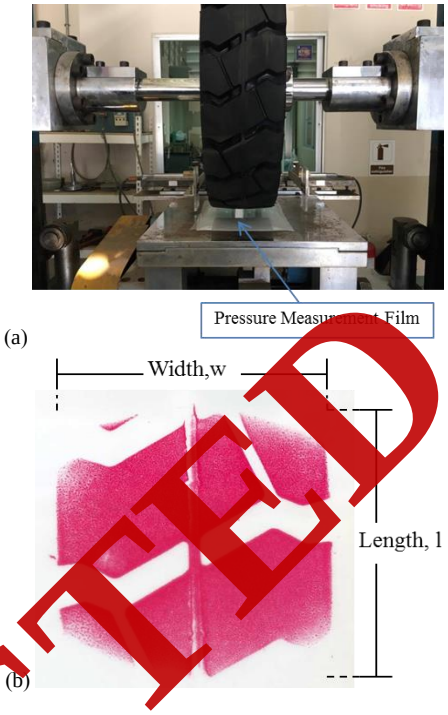

Figure 3. The tire stiffness testing: (a) compression test of a solid tire using the stiffness tester (EKTRON, model PL-2003) and (b) footprint on pressure measurement film

4. The Solid Tire Model

The 3D model of KOMACHI solid tire was constructed using digital data from the 3D scanner (Artec 3D, Eva) and SolidWorks software (Figure 4(a)). Each layer of solid tire was treated separately. The internal and middle layers of the solid tire model were meshed using hexagonal elements. The tread layer was meshed using tetrahedral elements. Then the internal, middle, and tread layers with the steel wires were built using 7,488, 4,320, 13,045, and 576 elements, respectively. The compound of the tread layer covered each side of the solid tire being placed on the sidewall. Figure 4(b) shows the finite element model of the KOMACHI solid tire. The properties for each layer of the solid tire model were described by the Ogden model (Phromjan & Suvanjumrat, 2018). The steel wires were specified with elastic modulus and Poisson's ratio of 200 GPa and 0.3, respectively. The elements of steel wire in internal, middle and inner tread layer were connected together with conjunct nodes, while the outer tread layer was connected with the inner tread by glue condition. This was validated by the material properties testing of the various rubber compounds. The solid tire rim was linked to the axial tire. This was to mimic the steel wheel fitting with the solid tire using multi-point constrains. To obtain the vertical displacements and footprint the model was arranged to contact a rigid floor. The friction coefficient is 0.8. This simulated the compression test. The tire axle was fixed and the rigid floor was moved up to press the solid tire model with the desired compression load. All finite element analyses of each compression load on the solid tire model were performed using MSC Marc software, which was installed in a personal computer with Core-i7 CPU and a RAM memory of 8 GB.

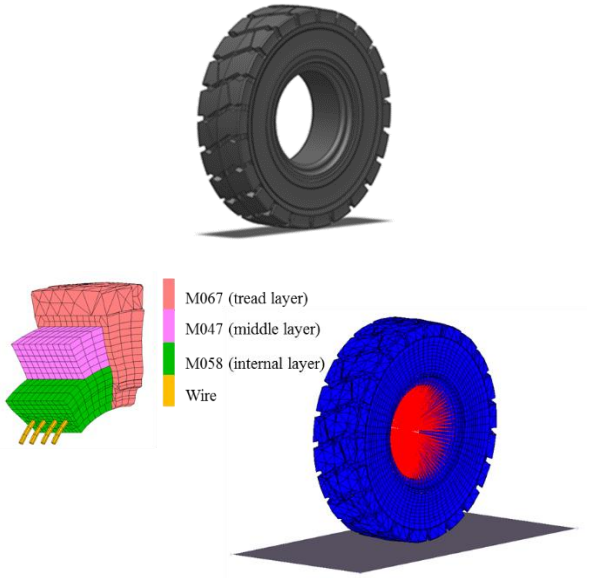

Figure 4. The KOMACHI solid tire model (a) 3-D model, and (b) finite element model

5. Results and Discussion

5.1 Constitutive modelling

The constitutive models of the three rubber compounds were determined by using curve fitting. The Ogden model was selected, and fit to the stress-strain curves of the rubber compounds. Figure 5 shows the curve fitting results of the Ogden constitutive model for the rubber materials M058, M047, and M067. These show good agreement with the stress-strain curves in all cases. So the Ogden model gave a very good description of the large strain behavior displayed by the rubber compounds. The curve fitting yielded the R^2 for the Ogden model as 0.990, 0.988, and 0.989 for the three rubber compounds. The compound M058 could support large compression loads with little deformation. The constants in the Ogden models fit to the stress-strain characteristics are shown in Table 2.

5.2 Vertical displacement analysis

The simulation results for compression tests of the solid tire are shown in Figure 6. The Von Mises stress and the vertical displacement are shown by color contours. The maximum value is yellow while the minimum value is blue. The largest deformation can be seen on the tire tread at contact with the rigid floor. Therefore, the maximum Von Mises stress was investigated at the tread of the model. This deformation behavior of the solid tire model was compared with actual physical experiments. Figure 7 shows the vertical deformation of both the solid tire model and the physical experiments at various compression loads. The vertical displacement increases linearly with the compression load. So, a solid tire model using the Ogden model for the material properties gives good agreement with the experimental data. The error of FEM when it was compared with the physical experiment at the compression loads of 4.0 kN, 5.0 kN, 6.0 kN, 8.0 kN, 10.0 kN and 12.0 kN was 16.90%, 15.05%, 12.21%, 18.76%, 10.37%, and 12.96%, respectively.

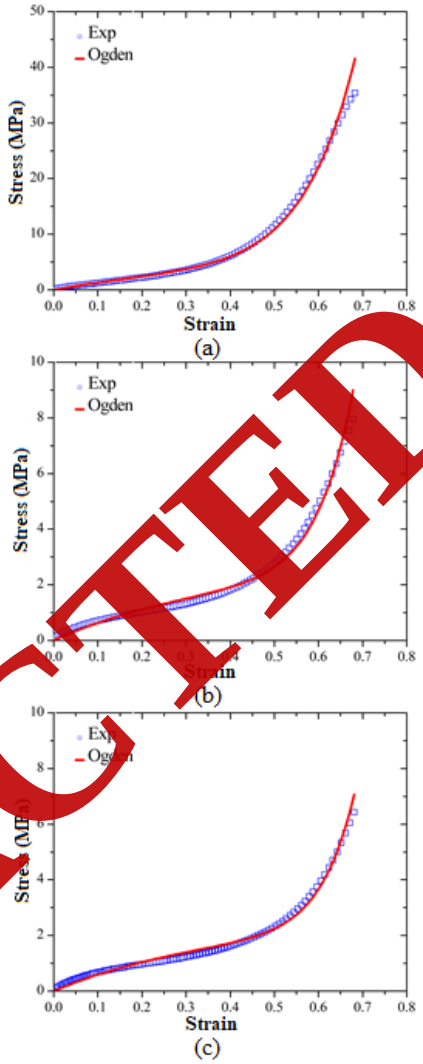

Figure 5. The curve fitting results using the Ogden model for rubber compounds (a) M058, (b) M047, and (c) M067

Table 2. The constants in fitted Ogden models

Rubber compound	Constants of the Ogden model				
	μ_1	μ_2	α_1	α_2	K
M058	5,646.43	0.019912	0.001682	15.4683	24,520
M047	0.00016	1,593.16	21.557	0.0031	12,171.8
M067	0.000045	1,273.06	23.379	0.0036	11,412.8

The layers inside the solid tire model were found to have different deformations because of the different stiffnesses of the rubber compounds used to build the KOMACHI solid tire. Figure 8 shows a section view of the model at the contact point when it is subjected to a compression load of 12.0 kN. It was found by FEA that the tread layer has the most deformation when the solid tire is under compression load. The model shows that the maximum stress occurs at the steel wire inside the solid

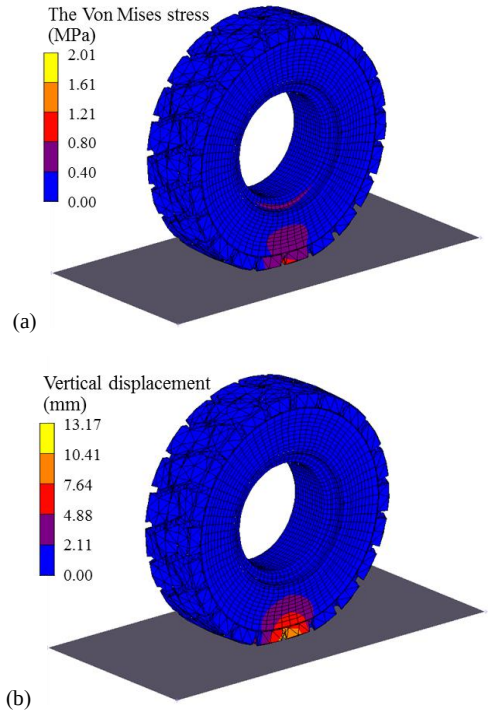

Figure 6. The simulation results, (a) Von Mises stress, and (b) vertical displacement, in compression test of solid tire at 12.0 kN load

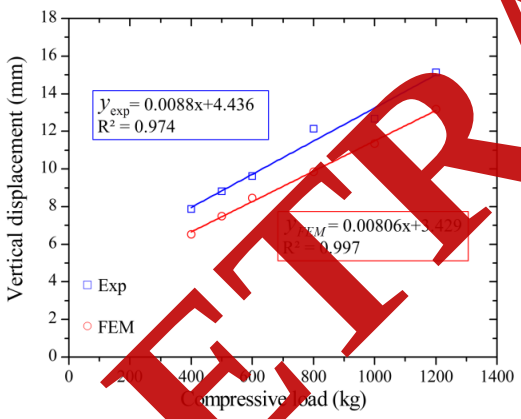

Figure 7. The vertical displacement vs. compression load in compression test of solid tires

tire. The ability to support heavy loads is a distinctive characteristic of the solid tire constructed from different rubber compounds. The internal layer is designed to be inflexible because it has to be fitted to the steel wheel of the forklift. Consequently, the color contour of the vertical displacement of this layer shows less deformation. The middle layer has been designed to support the impact load or to maximize the shock absorption when the solid tire is rolled on a rough floor. It was softer than internal layer. The tire tread has to have good contact and traction performance so the maximum strain occurred in the tread layer. The footprint characteristics on the rigid floor as simulated by the FEM show the traction performance. The tread performance of the solid tire will be described in the next section.

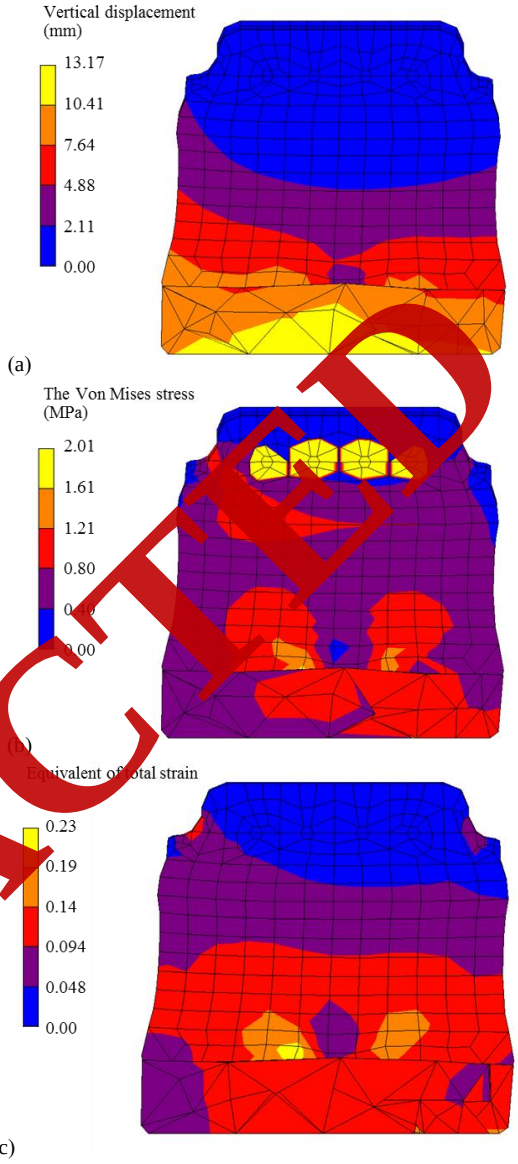

Figure 8. The simulation results, (a) vertical displacement, (b) stress, and (c) strain in compression test of a solid tire at 12.0 kN load

5.3 Footprint analysis

The footprints of KOMACHI solid tires from the whole tire experiments and from FEM model simulations were compared. Figure 9 shows the footprint when the solid tire is compressed by a heavy load. Color contours are used to express the contact pressure on the contact patch between the tire tread and the rigid floor. The geometric characteristics of the footprint comprise contact area, footprint area, contact area coefficient, tread contact length, tread contact width, coefficient contact, and footprint-shape coefficient (Chen, Guolin, Dengfeng & Yinwei, 2013). The footprint results of FEM are compared with the experimental results shown in Figure 9. Again, a color contour is used to indicate the contact pressure. The maximum is shown in red while the minimum is blue. The

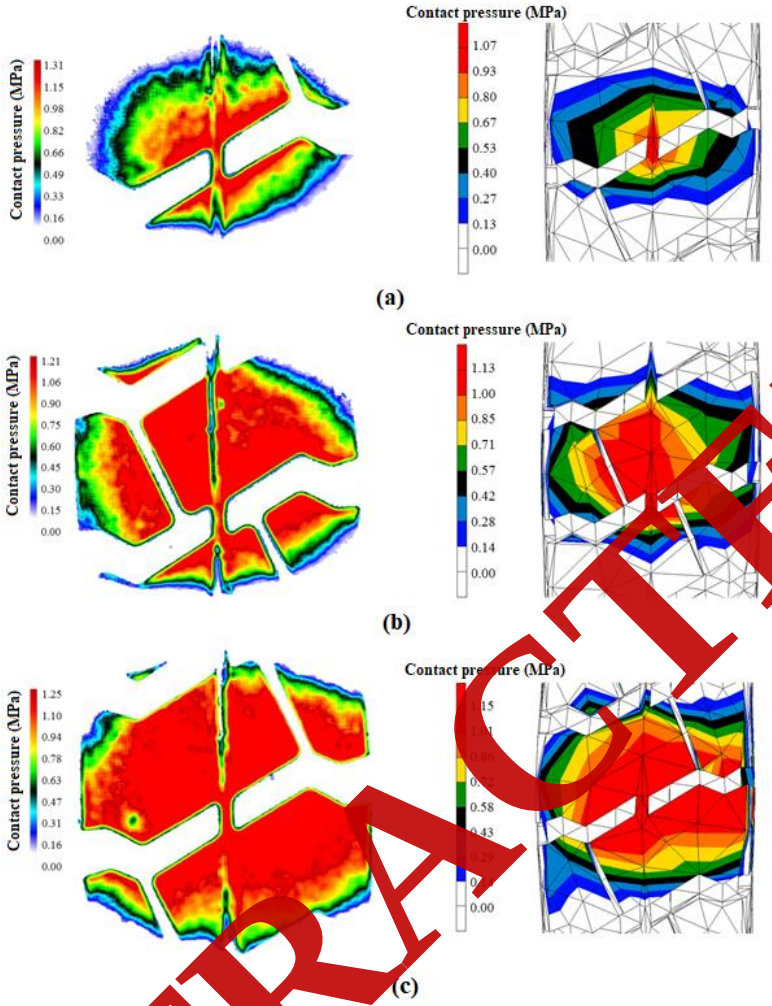

Figure 9. The footprint result comparison of experimental (left) and FEM simulation (right) in compression test of solid tire at (a) 4.0, (b) 8.0, and (c) 12.0 kN

footprint length, footprint width, footprint area, contact area, and contact pressure were measured. The footprint length increased little by little with compression load, while the footprint width also increased distinctly under compression loading. The footprint length and footprint width of compressed solid tire are presented in Figure 10(a) and Figure 10(b), respectively. The footprint areas under compression loading from the model are compared with those of the actual tire in Figure 10(c). Figure 10(d) compares the contact areas between FEM simulations and experiments. These areas increase with compression loading. However, the increase is less than that in the footprint area at the same compression. The contact pressure was calculated by dividing the contact force by the observed contact area of the footprint. A comparison of contact pressures is presented in Figure 10(e). The contact characteristics of the footprint obtained from the FEM were in good agreement with the experimental data. So, the FEM is a reliable predictor of the real tire footprint characteristics. The average errors of the FEM were less than 4.47%, 3.34%, 5.30%, 7.00%, and 11.07% when comparing footprint length, footprint width, footprint area, contact area, and contact pressure to the experimental data, respectively.

6. Conclusions

The rubber compounds used in a three-layer natural rubber solid tire have been examined for their stress-strain characteristics. These are the internal layer, the middle layer, and the tread layer of a solid tire. The stress-train curves were fit well by the Ogden model. The curve fits had R^2 of 0.990, 0.988 and 0.989, respectively. In stress-strain characteristics the internal layer was harder than the other two layers, while the tread layer was the softest.

The KOMACHI solid tires were subjected to compression testing at the six compression loads 4.0, 5.0, 6.0, 8.0, 10.0 and 12.0 kN. A solid tire model in FEM was constructed using tetrahedral and hexagonal elements. The Ogden model was assigned to the material properties of each layer. The properties of the model and those of the actual tire were compared across the compression loads. The vertical displacement showed a linear increase with compression loading and the simulations were in a good agreement with the real tire data. The FEM exhibited an average error of less than 14.38%.

The different layers of a solid tire experience different deformations. The internal layer is harder than the other

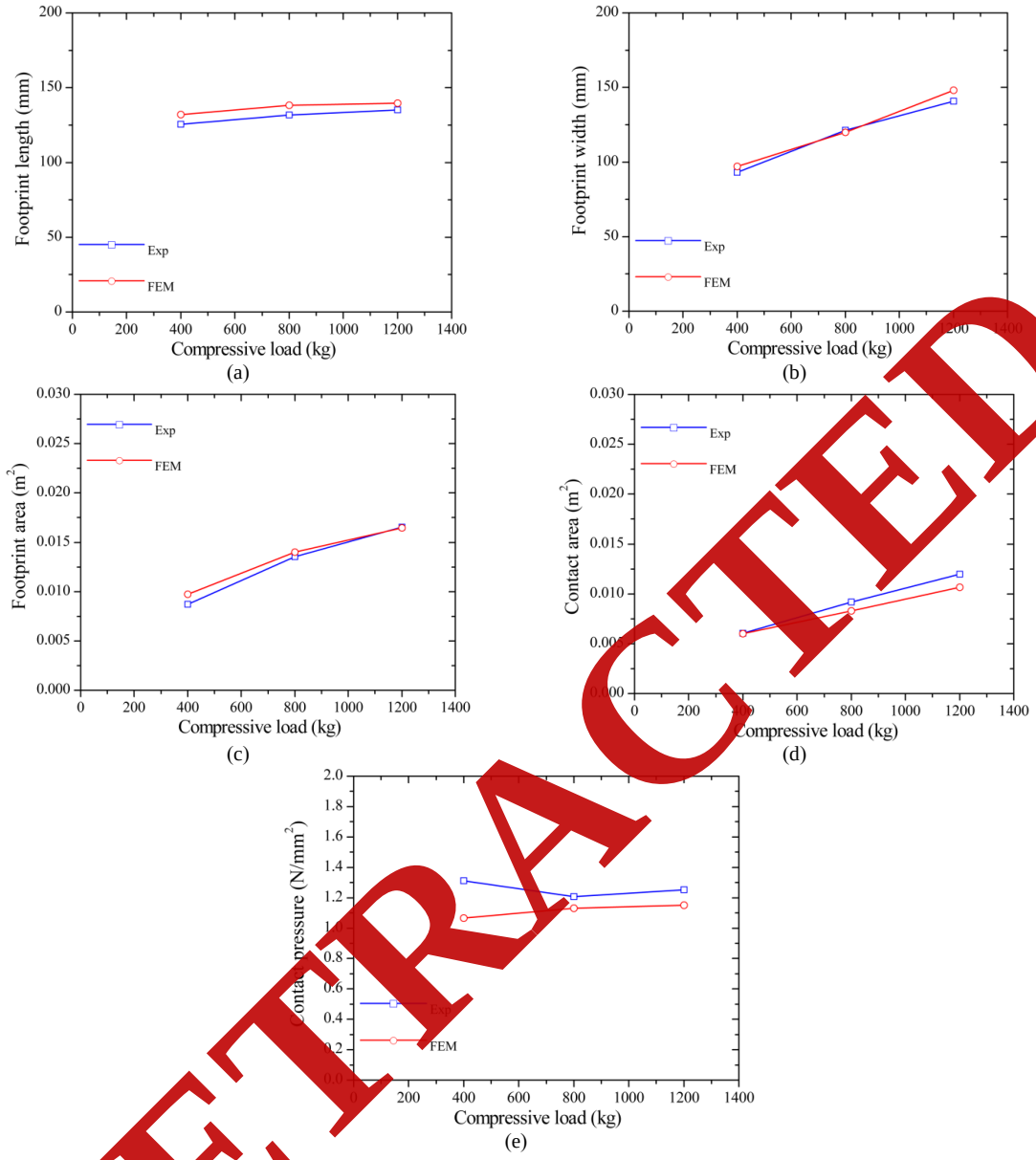

Figure 10. The footprint of compressed solid tire: (a) footprint length, (b) footprint width, (c) footprint area, (d) contact area, and (e) contact pressure under various compressive loads

layers because it has to fit securely to the forklift wheel. The deformation of the solid tire was investigated using FEA. The tread deformation was observed as the footprint. It was found that the footprint characteristics, length, width, area, and contact area, increased with the compression load. However, the contact pressures did not differ with increasing compression loading. The footprint characteristics obtained from the FEM agreed well with real tire data and had an average error of less than 6.24%. Consequently, the finite element model of a three-layer solid tire can be used for analysis of real tire performance. It was found that the Ogden model was applicable to the rubber components used in the solid tires. The finite element model developed in this research is advantageous for the design and development of solid tires.

Acknowledgments

This research was funded by The Thailand Research Fund (TRF) and V. S. Industry Tyres Co., Ltd under Research and Researchers for Industries (RRI) Master Scholarship (MSD59I0010).

References

Baranowski, P., Malachowski, J., Janiszewski, J., & Wwkwzer, J. (2016). Detailed tyre FE modelling with multistage validation for dynamic analysis. *Materials and Design*, *96*, 68-79.

Baranowski, P., Malachowski, J., & Mazurkiewicz, L. (2016) Numerical and experimental testing of vehicle tyre under impulse loading conditions. *International Journal of Mechanical Sciences, 106*, 346-356.

Baranowski, P., Janiszewski., & Malachowski, J. (2017). Tire rubber testing procedure over a wide range of strain rates. *Journal of Theoretical and Applied Mechanics, 55*(2), 727-739.

Bathe, K. J. (2014). *Finite element procedures* (2nd ed.). Massachusetts, MA: Pearson Education.

Behroozi, M., Olatunbosun, O. A., & Ding, W. (2012). Finite element analysis of aircraft tyre - Effect of model complexity on tyre performance characteristics. *Material and Design, 35*, 810-819.

Chen, L., Guolin, W., Dengfeng, A., & Yinwei, M. (2013). Tread wear and footprint geometrical characters of truck bus radial tires. *Chinese Journal of Mechanical Engineering, 26*(3), 506-511 (2013).

Guo, H., Bastien, C., Blundell, M., & Wood, G. (2014). Development of a detailed aircraft tyre finite element model for safety assessment. *Material and Design, 53*, 902-909.

Hassan, M. A., Abouel-Kasim, A., El-Sharief, M. A., & Yusof, F. (2012). Evaluation of material constants of nitrile butadiene rubbers (NBRs) with different carbon black loading (CB): FE-simulation and experimental. *Polymer, 53*(17), 3807-3814.

Li, X., Wei, Y., Feng, Q., & Luo, R. K. (2017). Mechanical behaivor of Nylon 66 tyre cord under monotonic and cyclic extension: experiments and constitutive modeling. *Fibers and Polymers, 18*(3), 542-548.

Mohsenimanesh, A., Ward, S. M., & Gilchrist, M. D. (2009). Stress analysis of a multi-laminated tractor tyre using non-linear 3D finite element analysis. *Material and Design, 30*(4), 1124-1132.

Namjoo, M., & Golbakhshi, H. (2015). An efficient design tool based on FEM for evaluating effects of components properties and operating conditions on interaction of tire with rigid road. *Journal of Central South University, 22*(1), 189-195.

Ogden, R. W. (1972). Large deformation isotropic elasticity: on the correlation of theory and experiment for incompressible rubberlike solids. *Proceeding of the Royal Society of London. Series A, Mathematical and Physical Sciences 326*(1567), 565-584.

Ogden, R. W. (1997). *Non-linear elastic deformation*. New York, NY: Dover Publication.

Phromjan, J., & Suvanjumrat, C. (2018). A suitable constitutive model for solid tire analysis under quasi-static loads using finite element method. *Engineering Journal, 22*(2), 141-155.

Yang, X., & Olatunbosun, O. A. (2012). Optimization of reinforcement turn-up effect on tyre durability and operating characteristics for racing tire design. *Material and Design, 35*, 798-809.

Wei, C., & Olatunbosun, O. A. (2016). The effects of tyre material and structure properties on relaxation length using finite element method. *Material and Design, 102*, 14-20.

Zhang, H., & Zhang, J. (2016). Static and dynamic sealing performance analysis of rubber D-ring based on FEM. *Journal of Failure Analysis and Prevention, 16*(1), 165-172.

Zhou, C., Zheng, J., Gu, C., Zhao, Y., & Liu, P. (2017). Sealing performance analysis of rubber O-ring in high-pressure gaseous hydrogen based on finite element method. *International Journal of Hydrogen Energy, 42*(16), 11996-12004.